Joint region-of-interest activity and alignment estimation in emission tomography

Johan Nuyts, Ahmadreza Rezaei
Nuclear Medicine, KU Leuven and Medical Imaging Research Center, KU Leuven, B-3000 Leuven, Belgium

***Abstract*— Previously, methods have been proposed for the direct reconstruction of the activity in a set of regions-of-interest (ROI), given the raw emission data and the locations of these ROIs in image space. These methods work well if the ROIs are well aligned, but artifacts may result if the alignment is poor. In this contribution, we propose a maximum likelihood reconstruction algorithm that estimates ROI-values where ROIs are available, and that applies standard voxel-based ML-reconstruction elsewhere. In addition, it jointly estimates the alignment of the ROIs to the image being reconstructed. The activity is updated with the standard MLEM update, the alignment with a least squares registration algorithm. A preliminary evaluation with simple 2D simulations and two microPET rat brain scans yielded promising results.**

I. Introduction

Several groups have studied the direct reconstruction of the activity within uniform regions-of-interest (ROI), as an alternative to standard reconstruction of voxels, followed by averaging over the voxels in the ROI [1]–[3]. ROI-reconstruction can be considered as an extreme case of reconstruction using anatomical side information, where penalties encourage smoothness within the anatomical boundaries, but not across the boundaries. If the underlying assumptions (well aligned ROIs and uniform tracer uptake inside each ROI) are valid then methods imposing smoothness or uniformity during reconstruction perform better than standard reconstruction, followed by post-processing [4]. The reason is that during reconstruction, the noise can be dealt with using the relatively simple Poisson model for the sinogram, whereas during post-processing, a noise model for the reconstructed image would be required, which is extremely complicated and therefore usually ignored. However, if the ROIs or anatomical boundaries are poorly aligned, artifacts may be produced. For that reason, methods have been studied to jointly estimate the activity and the alignment of the boundaries, e.g. [3], [5].

Here we propose a maximum likelihood (ML) algorithm for ROI-based reconstruction, given tomographic data and a set of ROIs that cover part of the object. The algorithm also estimates the alignment of the ROIs to the image being reconstructed. The activity is updated using the ML expectation maximisation (MLEM) or OSEM algorithm, the alignment is estimated with a dedicated registration algorithm.

II. Methods

The MLEM algorithm is designed to maximize the log likelihood function L given by

$$L = \sum_i y_i \ln \hat{y}_i - \hat{y}_i - y_i! \qquad \text{with } \hat{y}_i = \sum_j a_{ij}\lambda_j, \tag{1}$$

where y_i is the measured sinogram for line of response (LOR) i, λ_j is the estimated activity in voxel j and a_{ij} is the contribution of voxel j to LOR i. For (partially) ROI-based reconstruction, the likelihood (1) is rewritten as a function of the ROI-values $\boldsymbol{\rho}$ and the background values $\boldsymbol{\lambda^B}$ using

$$\lambda_j = \sum_n r_{jn}\rho_n + (1 - \sum_n r_{jn})\lambda_j^B \tag{2}$$

where $0 \leq r_{jn} \leq 1$ is the contribution of ROI n to voxel j (with $\sum_n r_{jn} \leq 1$) and λ_j^B is the background value for voxel j. The MLEM algorithm can then be used to reconstruct $[\boldsymbol{\rho}^T, (\boldsymbol{\lambda^B})^T]^T$ and the corresponding voxel image is computed with (2). Since λ_j^B is not estimated for voxels j that are entirely covered by one or more ROIs (i.e. $\sum_n r_{jn} = 1$), the total number of parameters to be estimated is less than in standard voxel-based MLEM.

Using a quadratic approximation for the likelihood in every iteration, the MLEM iteration can be well approximated as the maximisation of a separable quadratic surrogate function, constructed at that iteration [6]. Thus, in iteration h the image $\boldsymbol{\lambda}$ is updated as $\lambda_j^{(h+1)} = \lambda_j^{(h)} + \Delta\lambda_j$, where the update $\Delta\lambda_j$ can be regarded as the solution of

$$\frac{\partial}{\partial \Delta\lambda_j}\left(\sum_k \frac{S_k}{2}(\Delta\lambda_k)^2 + \dot{L}_k\Delta\lambda_k + c_k\right) = 0 \tag{3}$$

and therefore

$$\Delta\lambda_j = -\dot{L}_j/S_j. \tag{4}$$

Assuming now that a deformed activity image was already available, then one could maximize the surrogate function in every iteration by slightly deforming that available image $\boldsymbol{\lambda}$ using deformation parameters $\boldsymbol{\theta}$, which could be computed from

$$\sum_k (S_k\Delta\lambda_k(\boldsymbol{\theta}) + \dot{L}_k)\frac{\partial\Delta\lambda_k(\boldsymbol{\theta})}{\partial\theta_\xi} = 0. \tag{5}$$

where $\Delta\lambda_k(\boldsymbol{\theta})$ represents the change of the image due to deformation $\boldsymbol{\theta}$. Instead, one could apply a weighted least squares registration algorithm to register the current activity image to the image obtained by applying update (4), by minimizing

$$\sum_k w_k(\lambda_k + \Delta\lambda_k - (\lambda_k + \Delta\lambda_k(\boldsymbol{\theta})))^2, \tag{6}$$

Taking the derivative with respect to θ_ξ and inserting (4) one obtains

$$\sum_k \frac{w_k}{S_k}(S_k\Delta\lambda_k(\boldsymbol{\theta}) + \dot{L}_k)\frac{\partial\Delta\lambda_k(\boldsymbol{\theta})}{\partial\theta_\xi} = 0, \tag{7}$$

which is equivalent to (5) if the weights are chosen as $w_k = S_k$. Consequently, in an alternated likelihood maximisation, MLEM can be used to update the activity, while a weighted least squares registration algorithm can be used to update the deformation. This deformation is applied to the set of ROIs, which in turn causes a deformation of the ROI-based activity image. Since the background image does not have to be deformed, the registration is restricted to the ROIs by evaluating (6) only in voxels j that are part of a ROI, i.e. with $\sum_k r_{jk} > 0$.

III. Experiments

A simple 2D simulation was done, using a small Shepp-Logan like object embedded in a larger one. Fig. 1 shows the image of the true object and the MLEM reconstruction from the noisy sinogram. The first row of fig. 2 shows the original 5 ROIs representing the small object. With these ROIs, a ROI-based reconstruction (estimating ROI-values and background pixel values) without joint registration was done, shown in fig. 1. Finally, a ROI-based reconstruction with simultaneous estimation of an affine deformation of the ROIs was performed, shown in fig. 1 as well. The aligned ROIs are shown in fig. 2.

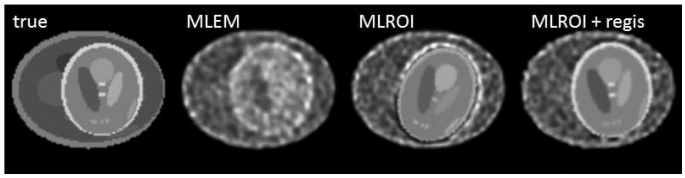

Fig. 1. From left to right: the phantom, MLEM-reconstruction, ROI-based reconstruction, joint ROI-based reconstruction and ROI-deformation.

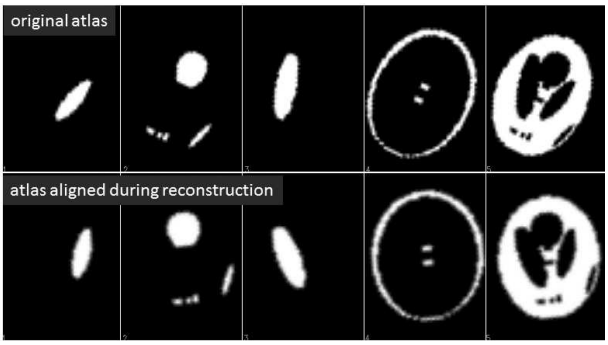

Fig. 2. The original set of ROIs (top row) and the same set after the affine registration, as estimated by the joint ROI-based reconstruction and ROI-deformation.

The method was also evaluated on a microPET brain scan of a rat after injection with [^{18}F]JNJ42259152, a ^{18}F-labeled tracer for PDE10A [7]. A set of 54 three-dimensional ROIs was derived from the digital atlas by Johnson et al [8]. The atlas provides 27 ROIs, but each ROI was split in a left and right part. An 89 min scan was started at the time of injection. A sinogram of the last 67 min. was reconstructed with MLEM (fig. 3). This tracer accumulates in the striatum but not in the rest of the brain. An image was created from the atlas by assigning a high value to the striatum, a low value to the rest of the brain and an intermediate value to the background. This image was registered to the MLEM reconstruction using normalized cross correlation, to have a first alignment of the atlas. Then the joint ROI-reconstruction/deformation was applied, using an affine registration with 9 degrees of freedom (translation, rotation and scale). The resulting image and ROIs are shown in fig. 3.

The method was applied to a 40 min dopamine transporter microPET scan of a rat after injection with [^{18}F]FECNT. As shown in fig. 4, this tracer accumulates in the striatum, but provides otherwise very little anatomical information. To produce an acceptable result, the ROI-deformation was restricted to a rigid one, because when scaling was allowed, the algorithm flattened the brain in vertical direction, making it about 70 % of its actual size. It is not yet clear why this happens.

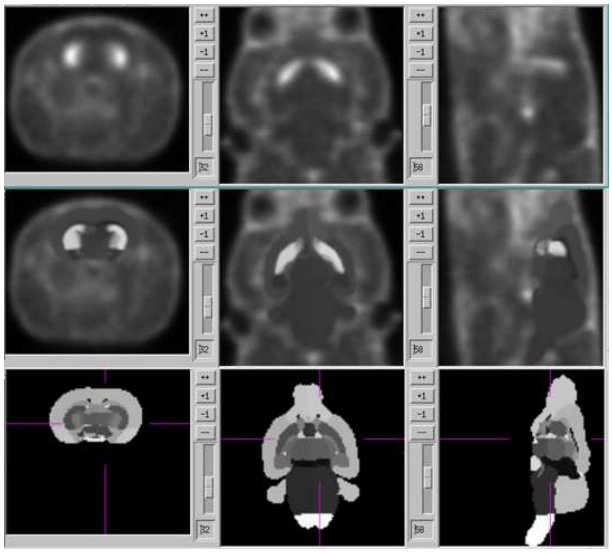

Fig. 3. Coronal, transaxial and sagittal slices through the MLEM image of the microPET scan with PDE10A tracer (top), the ROI-based reconstruction (center) and the corresponding deformed atlas (bottom). To display the atlas, arbitrary numbers were assigned to each of the ROIs.

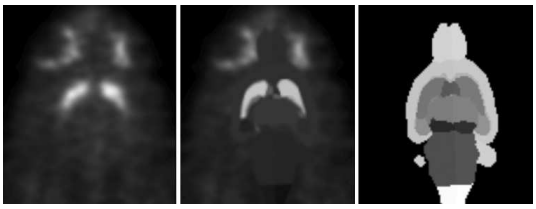

Fig. 4. Transaxial slice through the MLEM image of the microPET DAT scan (left), the ROI-based reconstruction (center) and the corresponding deformed atlas (right).

IV. Discussion

A ROI-based maximum likelihood algorithm is proposed, which uses standard MLEM or OSEM to update the activity estimates and a weighted least squares registration algorithm to update the deformation. Good results were obtained on 2D simulations and on a microPET rat scan. However, for another scan providing less anatomical information, a strong constraining of the deformation was required. Therefore, the robustness of the method needs further study.

V. Acknowledgement

The authors are grateful to Janaki Rangarajan, Cindy Casteels and Koen Van Laere for help with the atlas, and Terry Jones for an inspiring discussion about ROI-based reconstruction. This effort was supported by FWO research grant G027514N and by the KU Leuven research grant GOA/11/006.

References

[1] RE Carson, “A maximum likelihood method for region-of-interest evaluation in emission tomography”, *J Comput Assist Tomogr* 1986; 10; 654-663.

[2] RH Huesman, “A new fast algorithm for the evaluation of regions of interest and statistical uncertainty in computed tomography”, *Phys Med Biol* 1984; 29” 543-552.

[3] JE Bowsher, DM DeLong, TG Turkington, RJ Jaszczak, “Aligning emission tomography and MRI images by optimizing the emission-tomography image reconstruction objective function”, *IEEE Trans Nucl Sci*, 2006; 53: 1249-1258.

[4] J Nuyts, K Baete, D Bequé, P Dupont. “Comparison between MAP and post-processed ML for image reconstruction in emission tomography when anatomical knowledge is available.” *IEEE Trans Med Imaging* 2005; 24 (5): 667-675.

[5] Y Zhang, JA Fessler, NH Clinthorne, WL Rogers, “Incorporating MRI region information into SPECT reconstruction using joint estimation”, *ICASSP 1995*, vol 4, 2307-2310.

[6] K Van Slambrouck, J Nuyts. “Reconstruction scheme for accelerated maximum likelihood reconstruction: the patchwork structure”, *IEEE Trans Nucl Sci*, 2014; 61: 173-181.

[7] S. Celen, M. Koole, M. Ooms, M. De Angelis, I. Sannen, J. Cornelis, J. Alcazar, M. Schmidt, A. Verbruggen, X. Langlois, K. Van Laere, J.I. Andrés, G. Bormans. “Preclinical evaluation of [^{18}F]JNJ42259152 as a PET tracer for PDE10A”, *NeuroImage* 2013; 82: 13-22.

[8] GA Johnson, E Calabrese, A Badea, G Paxinos, C Watson. “Simultaneous reconstruction of activity and attenuation for PET/MR”, *NeuroImage*, 2012; 62: 1848-1856.